doi:10.1016/j.jmb.2004.02.033 *J. Mol. Biol.* (2004) **337**, 1109–1122

JMB

Available online at www.sciencedirect.com

SCIENCE DIRECT®

ELSEVIER

The ϕX174 Protein J Mediates DNA Packaging and Viral Attachment to Host Cells

Ricardo A. Bernal[1], Susan Hafenstein[2], Raquel Esmeralda[1] Bentley A. Fane[2] and Michael G. Rossmann[1]*

[1]*Department of Biological Sciences, Purdue University Lilly Hall, 915 W. State Street West Lafayette, IN 47907-2054 USA*

[2]*Department of Veterinary Science and Microbiology University of Arizona Building 90, Room 201, Tucson AZ 85721, USA*

**Corresponding author*

Packaging of viral genomes into their respective capsids requires partial neutralization of the highly negatively charged RNA or DNA. Many viruses, including the *Microviridae* bacteriophages ϕX174, G4, and α3, have solved this problem by coding for a highly positively charged nucleic acid-binding protein that is packaged along with the genome. The ϕX174 DNA-binding protein, J, is 13 amino acid residues longer than the α3 and G4 J proteins by virtue of an additional nucleic acid-binding domain at the amino terminus. Chimeric ϕX174 particles containing the smaller DNA-binding protein cannot be generated due to procapsid instability during DNA packaging. However, chimeric α3 and G4 phages, containing the ϕX174 DNA-binding protein in place of the endogenous J protein, assemble and are infectious, but are less dense than the respective wild-type species. In addition, host cell attachment and native gel migration assays indicate surface variations of these viruses that are controlled by the nature of the J protein.

The structure of α3 packaged with ϕX174 J protein was determined to 3.5 Å resolution and compared with the previously determined structures of ϕX174 and α3. The structures of the capsid and spike proteins in the chimeric particle remain unchanged within experimental error when compared to the wild-type α3 virion proteins. The amino-terminal region of the ϕX174 J protein, which is missing from wild-type α3 virions, is mostly disordered in the α3 chimera. The differences observed between solution properties of wild-type ϕX174, wild-type α3, and α3 chimera, including their ability to attach to host cells, correlates with the degree of order in the amino-terminal domain of the J protein. When ordered, this domain binds to the interior of the viral capsid and, thus, might control the flexibility of the capsid. In addition, the properties of the ϕX174 J protein in the chimera and the results of mutational analyses suggest that an evolutionary correlation may exist between the size of the J protein and the stoichiometry of the DNA pilot protein H, required in the initial stages of infection. Hence, the function of the J protein is to facilitate DNA packaging, as well as to mediate surface properties such as cell attachment and infection.

Keywords: bacteriophage α3; ϕX174; three-dimensional structure; DNA-binding protein; genome packaging

Present addresses: R. A. Bernal, Neurobiology Division, Medical Research Council, Laboratory of Molecular Biology, Hills Road, Cambridge, CB2 2QH, UK; S. Hafenstein, Department of Biological Sciences, Purdue University, Lilly Hall, 915 W. State Street, West Lafayette, IN 47907-2054, USA.

Abbreviations used: *amJ*, *amber J*; NCS, non-crystallographic symmetry; r.m.s., root-mean-square; ssDNA, single-stranded DNA; ssRNA, single-stranded RNA.

E-mail address of the corresponding author: mgr@indiana.bio.purdue.edu

Introduction

The assembly of viral proteins and nucleic acids into mature and biologically active virions involves a diversity of macromolecular interactions. After capsid formation, structural and packaging proteins must interact with viral nucleic acids. These interactions may confer packaging specificity, spatially organize the genome, enhance particle stability, or contribute directly to capsid quaternary structure.[1–4] Typically, packaging proteins are extremely basic, neutralizing the negative charges associated with the genome.[5–7] Many single-stranded RNA (ssRNA) plant viruses have capsid proteins with internally localized, basic N-terminal extensions that bind genomes non-specifically.[1,3,8–11] Interactions between the coat protein and the genome also have been observed in ssRNA animal viruses,[4,12] in single-stranded DNA (ssDNA) animal viruses,[13,14] and in ssDNA bacteriophages.[15] In the *Microviridae*, the ssDNA genome is associated with the inner surface of the capsid. Thus, alterations to either the protein or the genome can change the biophysical properties of the resulting virion.[16]

ϕX174, G4, and α3 are small, icosahedral, ssDNA bacteriophages belonging to the family *Microviridae*. The amino acid identity between the two most distantly related phages in this family, ϕX174 and α3, ranges from 72% in the F coat protein to 31% in the G spike protein. *Microviridae* contain up to 12 copies of the pilot protein H and 60 copies each of the coat protein F, the spike protein G, and the DNA-binding protein J.[17] The three-dimensional atomic structures of the ϕX174 and α3 virions, as well as their procapsid assembly intermediates, have been studied by X-ray crystallography and cryo-electron microscopy (cryoEM).[15,18–21] The F protein, forming the icosahedral capsid, is folded into the commonly found, eight-stranded, antiparallel β-barrel. Each of the 12 pentagonal vertices is decorated by a pentamer of protein G. The hydrophilic channel formed along the 5-fold axes of G and F may be the exit route of the DNA during infection.[19] Protein J binds to and is packaged with the viral ssDNA.[22,23] Subsequently, it binds to the internal surface of the capsid, displacing the internal scaffolding protein B, which occupies a similar position in unfilled procapsids.[20] Binding of J protein to the coat protein and the genome effectively tethers the genome to the inner surface of the capsid. After genome packaging into the procapsid, the 240 copies of the external scaffolding protein are shed during provirion to virion maturation (Figure 1).

The ϕX174 DNA-binding protein J is divided into three functional parts: the 13 residue amino-terminal domain 0, the 15 residue middle domain I, and the nine residue carboxy-terminal domain II (Figure 2). Domains 0 and I are highly basic with many positively charged residues in each region. In contrast, domain II is very hydrophobic and contains no basic residues. Domain 0, which makes extensive contacts with the inside of the ϕX174 capsid, binds to the neighboring F subunit, as compared to the location of domains I and II.[15] In other *Microviridae*, the J protein consists of only domains I and II. Domain I of the α3 J protein has a structure that is rather different from that of the J protein in ϕX174, with a root-mean-square (r.m.s.) deviation between equivalent C^{α} atoms of 4.8 Å. Nevertheless, domain I of J for both viruses binds to essentially the same position on the inside of the capsid. In contrast, the structure of the hydrophobic domain II is similar in ϕX174 and α3,

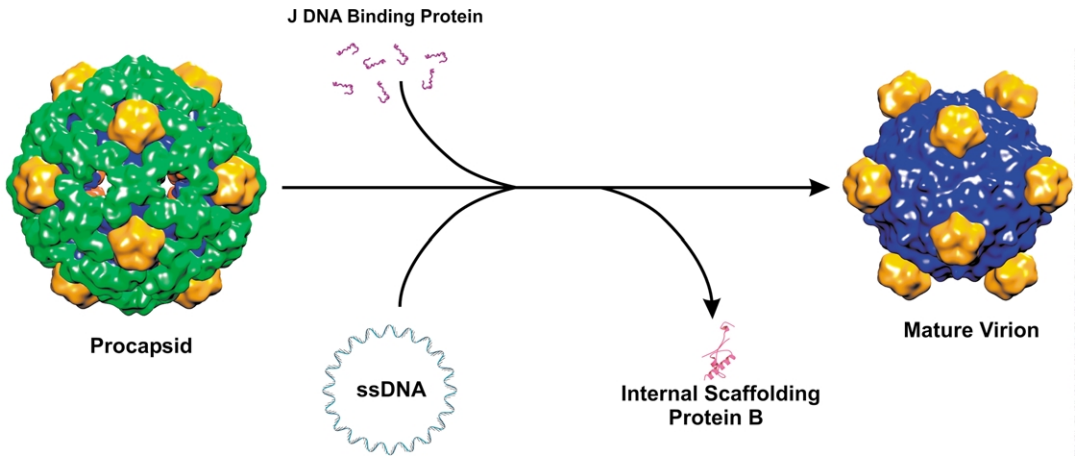

Figure 1. *Microviridae* assembly pathway. The internal scaffolding protein B (shaded red, and barely visible) and external scaffolding protein D (shaded green) are required for the assembly of pentameric intermediates into an empty protein shell called the procapsid.[45–47] The F capsid protein is shaded blue, and the G spike protein is shaded yellow. The ssDNA is concurrently synthesized and packaged along with the basic DNA-binding protein J, which displaces the internal scaffolding protein B by competition for the same hydrophobic binding pocket on the internal surface of the F capsid protein.[21] The resulting particle, or provirion, sheds the external scaffolding protein lattice to form the mature virion.

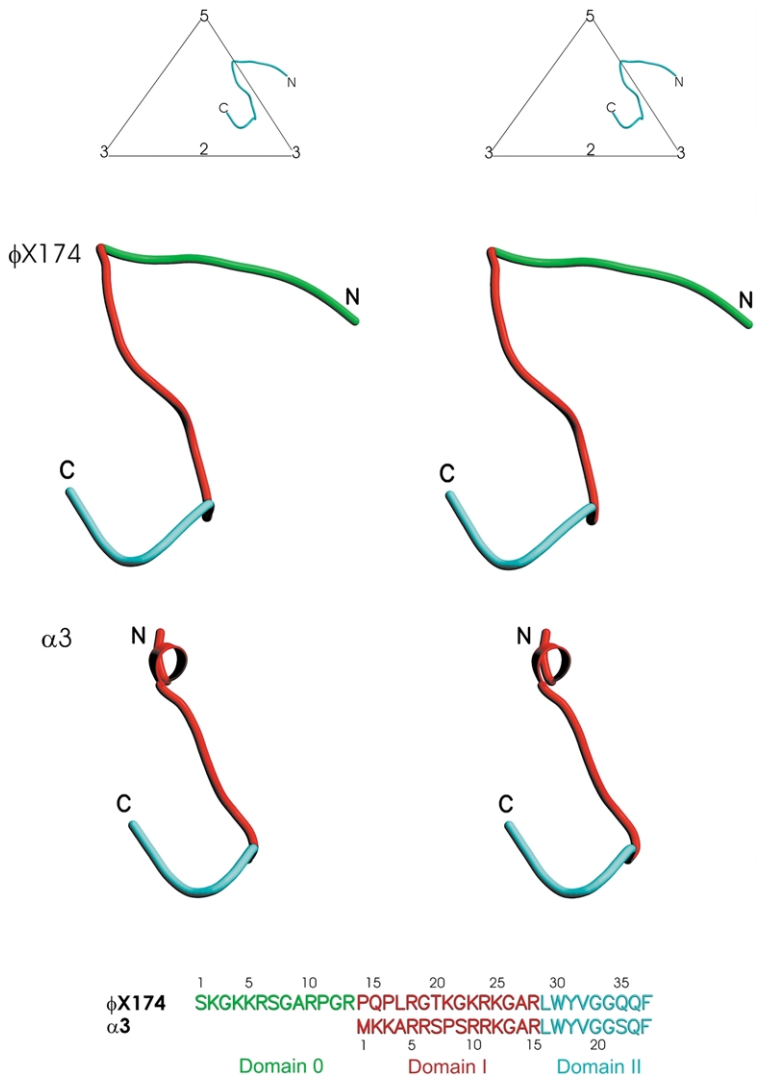

Figure 2. Comparison of the ϕX174 J protein structure (top structure) with that of the α3 J protein (bottom structure). The three functional regions are highlighted: green, domain 0; red, domain I; and blue, domain II. The sequence alignment is color-coded to match the structures. The only secondary structure in the J protein is found in α3 in the form of a one-turn α-helix. The inset above the structures gives the position of the J protein relative to the symmetry axes.

with the r.m.s. deviation being only 0.5 Å between equivalent C^{α} atoms.

In some viruses, including ϕX174 and α3, the capsid has imposed some degree of its icosahedral symmetry onto the genome.[18,19] Domain I and part of domain II are associated with icosahedrally ordered DNA in the X-ray structures of *Microviridae*. The icosahedrally ordered DNA is in roughly the same location in both the ϕX174 and α3 viruses.[18,19] The results of previous studies, in which the association of the genome with the inner surface of the capsid was altered by packaging with mutant J proteins, suggested that these internal alterations influence the outer surfaces of the capsid.[16,24] In order to determine how different wild-type J proteins affect DNA packaging and the properties of the virus, chimeric *Microviridae* particles were produced by packaging α3 and G4 with the ϕX174 DNA-binding protein. The resultant chimeric virions were characterized by a variety of criteria, such as buoyant density, native gel migration rate, host cell attachment efficiency, and X-ray structure determination. These observations suggest that the binding of domain 0 to the inside of the capsid affects the flexibility of the virions.

Results

The biological and solution properties of the chimeric particle

To eliminate the expression of endogenous DNA-binding proteins, *amber J* (*amJ*) mutations were placed into the ϕX174, α3, and G4 genomes. Thus, propagating an *amJ* mutant within the cell line harboring a clone of a wild-type foreign J gene allowed assembly of virions with foreign J proteins.[25] In plaque assays (Table 1), it was found that the longer J protein of ϕX174 could substitute for the shorter J proteins in α3 and G4. However, the shorter J proteins of α3 and G4, which lack domain 0, could not replace the ϕX174 J protein.

The buoyant densities of α3 and ϕX174 were compared to the buoyant density of the chimeric α3 particles formed by packaging α3 with the

Table 1. Cross-functional analysis of *Microviridae* J genes

Mutant	Efficiency of plating[a] on BAF30 (*recA*)[b] with			
	pϕXJ	pG4J	pα3J	No plasmid
ϕX174 *amJ*	1.0	1.0×10^{-6}	1.0×10^{-6}	1.0×10^{-6}
G4 *amJ*	1.0	1.0	0.7	2.0×10^{-6}
α3 *amJ*	1.5	1.0	1.0	3.0×10^{-5}

[a] Restrictive titer/permissive titer, as determined on BAF30 (*recA*) containing a plasmid expressing the same J gene.
[b] BAF30 is a *recA*-null derivative of C122 (sup^0) wild-type host.

ϕX174 DNA-binding protein J. All three types of particles were assayed in the same gradient using genetic markers to identify the virion type in each fraction. The chimeric particles were found to have a buoyant density intermediate between the two wild-types. The density difference between the chimeric and wild-type α3 virions was of the order of 1.5%. For both chimeric and wild-type α3 virions, a minor peak of less dense particles was detected (Figure 3). The magnitude of the density differences is the same for chimeric and wild-type α3 particles. In contrast, the sub-population peak of wild-type ϕX174 is of greater density than the major ϕX174 population. Similar results were obtained in experiments comparing wild-type G4 and chimeric particles packaged with ϕX174 J protein.

The migration rates of chimeric and wild-type virions were analyzed in bidirectional, native agarose gels, which assay for differences in size and charge, presumably on the surface.[16,26] The α3 wild-type particles were found to migrate faster than ϕX174 virions, with the chimera intermediate between the two (Figure 4).

Host cell attachment efficiency was assayed by determining the number of unattached virions remaining in the supernatant at progressive time-points.[16] The α3 wild-type particles attach less well than ϕX174 virions, by three orders of magnitude. Again, the chimeric particles exhibited an intermediate efficiency (Figure 5).

The structure of the F capsid and G spike proteins in the chimeric virus

Both the F and G proteins of the chimeric virion have an r.m.s. deviation of less than 0.3 Å when compared to the structure of the wild-type α3 virus by superimposing the icosahedral symmetry axes (Table 2). Furthermore, the r.m.s. deviation is

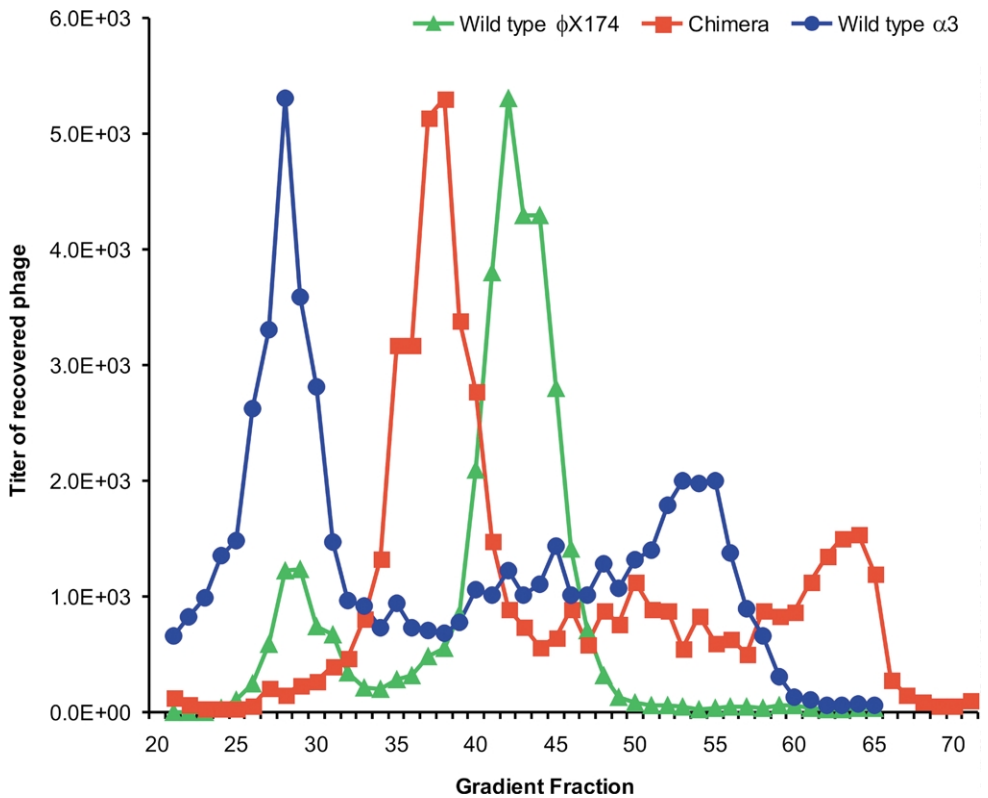

Figure 3. Buoyant densities of wild-type ϕX174, chimera, and wild-type α3. All three types of particles were analyzed within the same gradient. The chimera was propagated by growing an α3 *amJ* mutant in a *recA* cell line harboring an inducible clone of the ϕX174 J gene. An additional genetic marker, *amB*, was placed in the wild-type α3 background, and an *amD* mutation was placed as a marker in the wild-type ϕX174 background. This allowed the particles to be distinguished by titering on different cell lines harboring specific expression vector clones. Particle titers were normalized to the same order of magnitude for the graph.

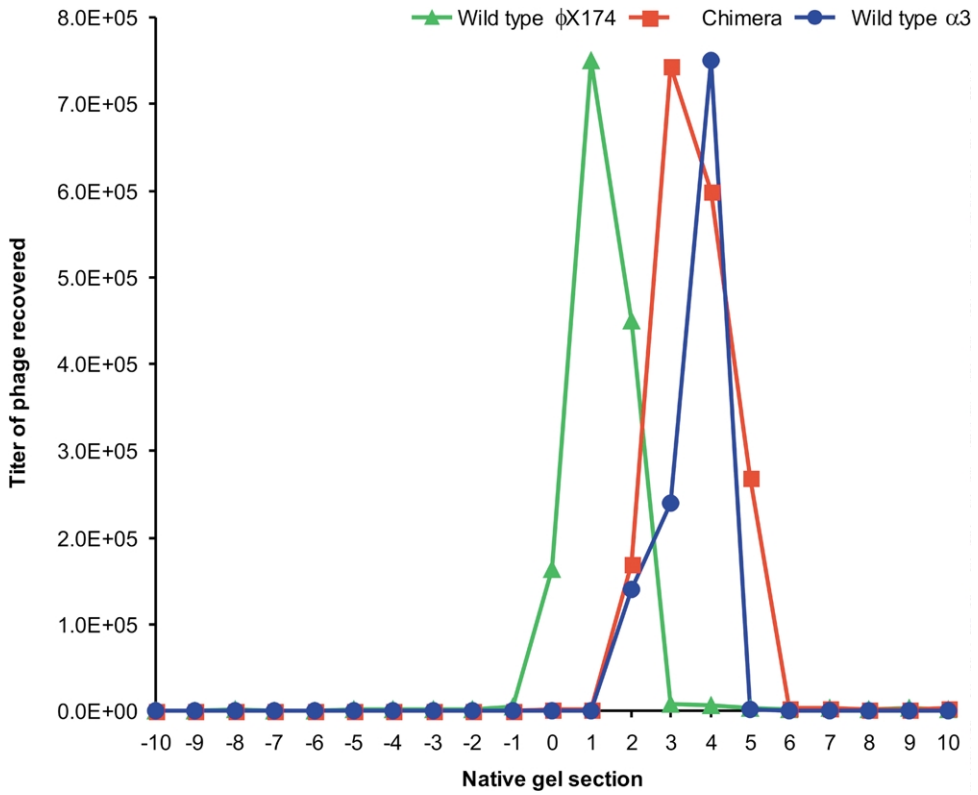

Figure 4. Native gel migration of wild-type ϕX174, chimera, and wild-type α3. Negative gel section numbers indicate movement toward the (−) electrode; positive gel section numbers indicate movement toward the (+) electrode. Each section is approximately 2 mm in length.

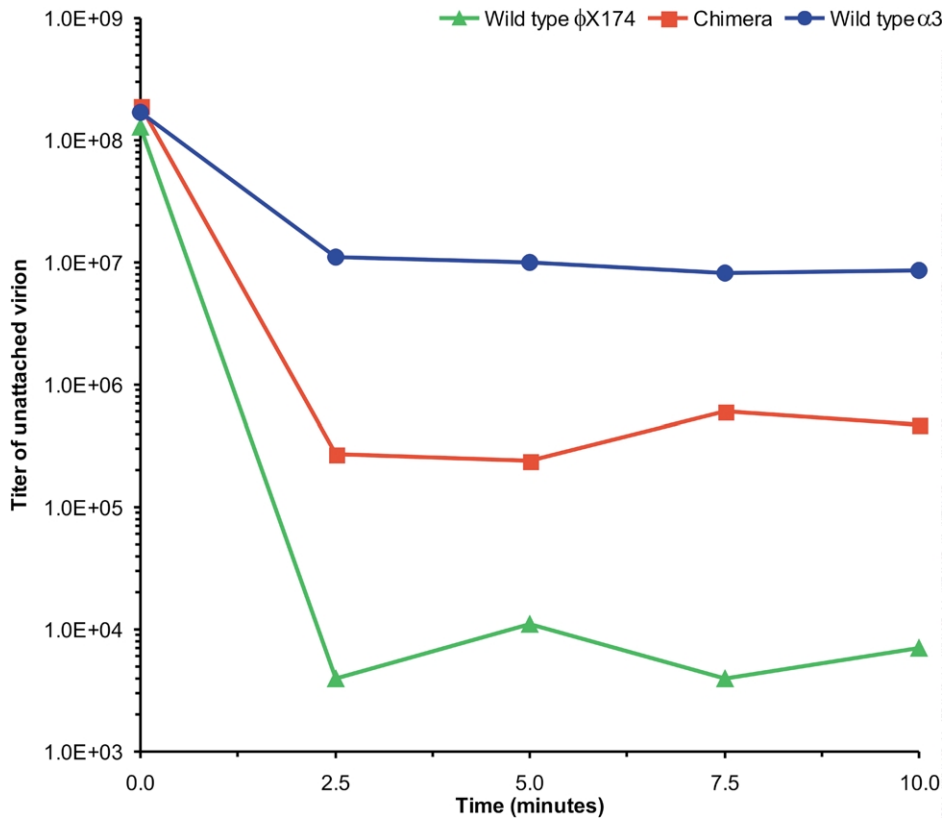

Figure 5. The attachment efficiency of wild-type ϕX174, chimera, and wild-type α3 particles. Efficiency was assayed as the titer of unattached virion at progressive time points.

Table 2. r.m.s. deviation (Å) between equivalent C^{α} atoms of ϕX174 and α3 when superimposed by aligning the icosahedral axes

Protein	α3	ϕX174
α3 Chimera F	0.229	0.901
α3 Chimera G	0.349	2.482
α3 Chimera J	2.605	0.782
ϕX174 F	0.812	–
ϕX174 G	2.358	–
ϕX174 J_{Whole}	3.116	–
ϕX174 $J_{C\text{-}term}$	0.494	–

only 0.6 Å between equivalent α3 and ϕX174 C^{α} atoms for residues whose side-chain atoms approach the J protein to within 3.4 Å. Thus, the presence of the foreign ϕX174 J protein in the chimeric virus had no measurable effect on the conformation of either the capsid or the spike proteins.

The structure of the J protein in the chimeric virus

The DNA-binding protein J is situated at the interface between the internal surface of the capsid and the nucleic acid. Although the ϕX174 J protein has a similar conformation in its indigenous and foreign environments, the parts that would not have existed in α3 are mostly disordered. Specifically, residues 1–8 in domain 0 and residues 22–24 in domain I (Tables 3 and 4, Figures 2 and 6) are disordered in the J protein in the chimera. This is surprising, because the residues in the coat protein that make contact with domain 0 in ϕX174 are completely conserved in α3, leading to the expectation that domain 0 of the J protein in the chimera would also be ordered.

Domain I of the J protein in the chimera follows closely the C^{α} backbone found in ϕX174 (r.m.s. deviation of 0.9 Å) and, hence, differs from the structure of the α3 J protein. The majority of the differences are limited to a single α-helical turn in the wild-type α3 J protein and to the side-chains. Domain I straddles the interface between 5-fold related F proteins (Table 4) and domain II is very similar in all three particle types (Table 5).

Ordered nucleic acid structure

The partially icosahedrally ordered nucleic acid

Table 3. Contacts between protein F and domain 0 of protein J

Protein J residues			Number of polar, van der Waals, and hydrophobic interactions with residues in protein F[a]											
			ϕX174				Chimera				α3			
ϕX174	Chimera	α3	Res.	P	V	H	Res.	P	V	H	Res.	P	V	H
K2			**L236**	1	4	1								
			V237	0	2	0								
G3			**L236**	1	1	1								
			V237	1	2	1								
			M238	0	2	2								
			R239	0	1	0								
K4	K4		**M238**	0	1	1								
			R239	0	3	0								
K5	K5		**M238**	0	2	1								
			R239	0	2	0								
R6	R6		**R239**	1	1	0								
			S240	0	0	5								
			N241	0	6	4								
S7	S7		**S240**	0	1	0								
			K269	1	2	0								
G8	G8		**L242**	0	2	3								
			T267	0	3	0								
			Y268	1	2	3								
			K269	0	1	1								
R10	R10		**V46**	0	2	0	**T268**	1	2	0				
			T267	1	3	2								
			K269	0	10	2								
G12	G12		**T267**	0	2	0	**T268**	0	1	0				
			Total	7	55	27	Total	1	3	0	Total	0	0	0

Bold type indicates symmetry-related proteins. Selection criterion based on a distance of 3.6 Å.
[a] Res., residue; P, polar; V, van der Waals; H, hydrophobic.

in the α3, ϕX174, and α3 chimeric structures is located in a basic pocket on the inner surface of protein F that is partially occupied by the J protein (Figure 7). The structure of the four nucleotides previously identified in ϕX174[19] required only minor adjustments to be fit into the density of the chimeric and α3 viruses. The sugar-phosphate backbone for six additional nucleotides was also visible near the carboxy terminus of protein J, but differed in position for the chimeric and α3 virions. However, the ordered ssDNA lacks the phosphodiester backbone of conventional *B*-type backbone geometry and base-stacking. The icosahedrally ordered DNA has roughly the same location in all three particles. The smaller number of bases recognized in the 3 Å resolution map of ϕX174[19] may be because this map was interpreted ten years before the α3 and chimeric structures were interpreted. In the intervening decade, experience has been gained for interpreting the density associated with semi-ordered nucleic acids.[13]

Discussion

Comparison of the chimera with wild-type α3 shows that the chimera is less dense than wild-type. Yet, the chimeric virus contains 60 copies of the larger ϕX174 J protein with 13 extra residues in each copy. Thus, if the F capsid protein were of the same size in both the chimeric and wild-type viruses, then the chimera would have an additional 92 kDa mass, an increase of 1.5% in molecular mass over that of wild-type α3. However, the density of the chimeric virus is not greater, but actually 1.5% less than the density of the wild-type virus (Figure 3). The observed buoyant density differences could possibly be the result of cesium ions binding to the external surface of the capsid or binding to internal sites. However, cesium had been ruled out previously as an interfering factor in buoyant density determination of *Microviridae*.[16,24] Hence, the volume of the chimeric virus must be greater by about 0.5% or the radius by 0.7 Å. Such a small change in radius is on the

Table 4. Contacts between protein F and domain I of protein J

Protein J residues			Number of polar, van der Waals, and hydrophobic interactions with residues in protein F[a]											
			ϕX174				Chimera				α3			
ϕX174	Chimera	α3	Res.	P	V	H	Res.	P	V	H	Res.	P	V	H
P14	P14		**Q265**	0	0	1	**Q266**	0	2	2				
P16	P16	K3	D61	0	0	1	D62	0	2	0	**R412**	0	1	0
L17	L17	A4	A59	1	1	0	D62	1	1	0	**L18**	0	1	0
			I60	0	3	0	I61	0	2	0	**Q410**	0	1	0
			D61	1	0	0	**A411**	0	2	1				
R18	R18	R5	D61	1	2	0					I61	0	4	0
			W243	0	3	2					D62	1	2	1
G19	G19	R6	**K407**	1	2	0	W244	0	4	2	D62	2	0	0
							R412	2	1	0	W244	0	1	3
											R412	1	0	0
T20		S7	**H16**	0	1	0					**L18**	0	1	2
			L17	1	1	3					**W244**	0	2	0
			S356	0	1	0					D357	0	2	0
			K407	0	1	1								
K21	K21	P8	**D13**	0	1	0	**D14**	0	1	0	**H17**	0	1	1
			K407	1	4	0	**R412**	0	3	0	**R412**	0	0	1
G22	G22		**D13**	2	2	1	**S16**	0	1	1				
			S15	1	2	1	**R412**	1	2	0				
			K407	1	1	0								
			N409	0	3	0								
K23		R10	**D44**	1	0	0					**D14**	0	2	0
											S16	2	1	0
											H355	1	0	0
											D357	1	0	0
R24	R24		**P11**	0	2	0								
			D13	0	1	0								
			Y413	2	3	1								
		K12									**D14**	0	1	0
	R28	R15					V424	0	1	0	**V424**	0	1	0
			Total	13	34	11	Total	4	22	6	Total	8	21	8

Bold type indicates symmetry-related proteins. Selection criterion based on a distance of 3.6 Å.
[a] Res., residue; P, polar; V, van der Waals; H, hydrophobic.

borderline of detection by X-ray crystallography, considering the uncertainty of the assumed wavelength at the synchrotron source when the data were being collected. The assumed wavelength of 1.0 Å would have had to be in error by only 0.005 Å.

There are other indications that the virus has changed shape. For instance, the attachment efficiency of the chimeric particles is two orders of magnitude higher than that of wild-type α3 (Figure 5), suggesting surface changes. These changes might be either in altering the assembly of a unique particle type or in affecting the ratio of fast and slow-adsorbing species, which may be indicated by the presence of both major and minor sedimenting bands in buoyant density gradients (Figure 3). Changes in surface features are indicated also by differences in migration rates in native gels (Figure 4). Changes in surface structure would be consistent with changes in virus volume. However, structural changes resulting from corresponding differences in volume would be too small to be observed at the resolution of the chimera structure. Nevertheless, there are major structural differences that reside in domain 0 of the J protein and these are, therefore, presumably responsible, directly or indirectly, for the changes in the surface properties and buoyant densities of the viruses.

Domains I and II of each of the 60 J proteins are situated in a deep channel along the interface of adjacent capsid proteins on the inside of the virion. The channel is a conserved feature that is found in *Microviridae*, forming a basic environment. It is surprising, therefore, that, in light of the very basic character of J itself, this protein binds into the channel. However, there is an increase in the basic character of the channel when J is bound there, presenting a surface highly suitable for DNA binding. Furthermore, this is the region where partially ordered DNA is found. Domain 0 binds to a somewhat more exposed region of the inside of the virion and to a slightly less basic surface.

The amino acid residues that participate in binding domain 0 to the F protein in wild-type ϕX174 are nearly all conserved between the F capsid proteins of ϕX174 and α3. Hence, it might be expected that the interactions of domain 0 with the interior of the capsid shell in wild-type ϕX174 and in chimeric α3 would be much the same. However, domain 0 is fully ordered only in the ϕX174 capsid; it is mostly disordered in the α3 capsid. The protein and DNA content of the ϕX174 and α3 capsids are considerably different. Whereas the genome of α3 is bigger by 681 bases, there are only about five H protein molecules (331 amino acid residues each) in α3 as opposed to about ten H protein molecules (328 amino acid residues each) in ϕX174. Furthermore, the additional 13

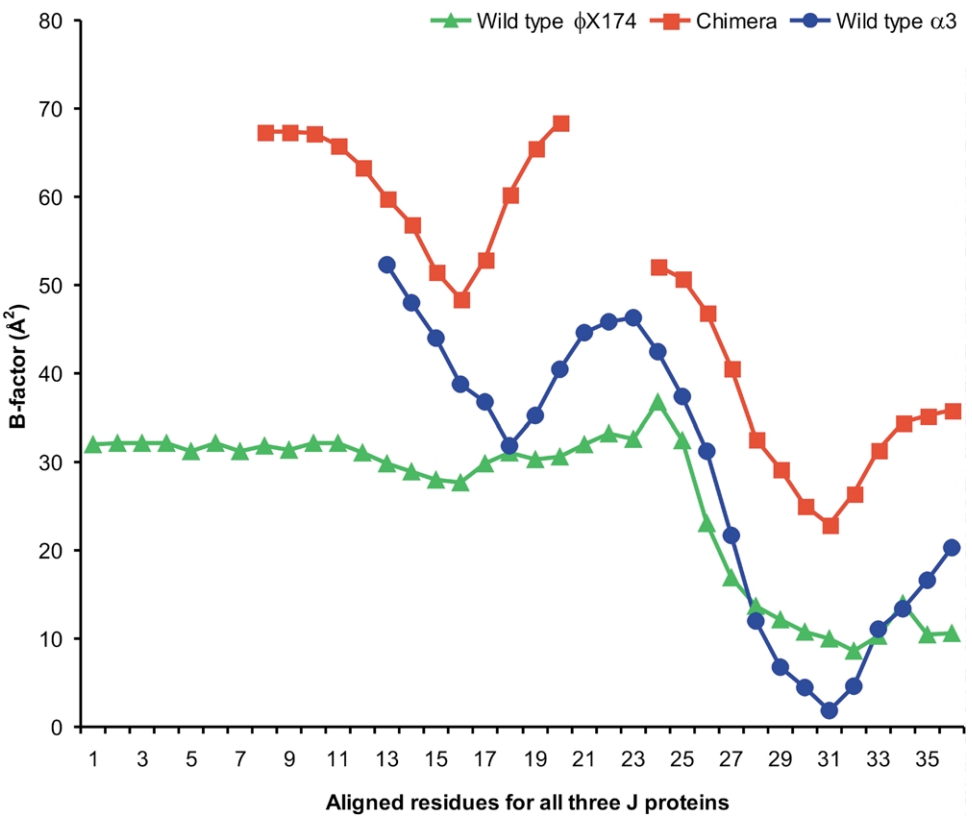

Figure 6. Temperature factor comparison of the wild-type ϕX174, chimera, and wild-type α3 proteins. The temperature factor, *B*, for each C^{α} atom is plotted on the *y* axis with equivalenced residue numbers on the *x* axis.

residues in each of the 60 J molecules add another 780 amino acid residues to the content of ϕX174. Thus, in total, there are approximately an additional 2420 amino acid residues in the ϕX174 capsid as opposed to the extra 681 bases in α3. Hence, overall there is considerable crowding in ϕX174 compared to α3.

Domain 0 may be related to the number of DNA pilot proteins H incorporated per capsid. ϕX174 requires 10–12 H proteins for infectivity. Fewer copies result in defective particles that lose DNA from the 5-fold vertices during packaging.[27] Bacteriophage α3, on the other hand, is infectious with only six copies of protein H. Attempting to fill ϕX174 with a smaller DNA-binding protein causes procapsids to dissociate during packaging.[25] Mutations in the C terminus of the α3 DNA-binding protein inhibit virion maturation, but are suppressed by substitutions in protein H.[28,29] Presumably, particle stability can be affected by altering the structure of the pilot protein. Therefore, the more stringent H protein requirement in ϕX174 may necessitate a more elaborate DNA-binding protein, one capable of guiding DNA away from vertices containing the H proteins.

The H protein content of the chimera was examined and found not to differ from wild-type α3 (data not shown). Hence, the lack of crowding in the chimera may account for the ability of domain 0 to have numerous conformations, giving rise to a disordered structure, whereas in ϕX174 domain 0 is held against a weak binding surface. The tighter binding of domain 0 to the F capsid protein in ϕX174 might reduce the flexibility of the capsid in a manner equivalent to binding of a "pocket factor" to the capsids of rhinoviruses.[30] Therefore, binding of domain 0 may reduce the flexibility of ϕX174 as opposed to α3. The chimera structure would be intermediate in that not quite all of domain 0 is disordered, there being diffuse electron density and a high mean temperature factor (Figure 8) for residues 9–13 of the J protein

Table 5. Contacts between protein F and domain II of protein J

Protein J residues			Number of polar, van der Waals, and hydrophobic interactions with residues in protein F[a]											
			ϕX174				Chimera				α3			
ϕX174	Chimera	α3	Res.	P	V	H	Res.	P	V	H	Res.	P	V	H
L29	L29	L16	Q349	0	1	0	**V424**	0	1	1	**V424**	0	1	0
			R352	0	1	0								
			T419	0	1	0								
W30	W30	W17	K166	0	0	2	N168	0	1	1	N168	0	0	1
			N167	0	3	0	I169	0	1	0	I169	0	1	1
			I168	0	1	0	A172	0	1	0	I350	0	0	1
			A171	0	1	0								
			Q349	0	1	0								
Y31	Y31	Y18	P174	0	1	0	P173	0	1	0	L174	0	1	0
			F211	0	0	3	**V424**	0	0	2	R425	0	1	0
							R425	0	1	0				
V32	V32	V19	P138	0	0	0	P139	0	1	0	P139	0	1	0
			W139	0	0	0	W140	0	1	0	W140	0	1	0
							Y211	1	0	0				
G33	G33	G20	P138	0	0	0	Y211	2	2	0	T210	0	1	0
			D209	0	0	0	F212	0	1	2	Y211	1	1	0
			Y210	0	0	0	M213	1	0	0	F212	0	2	0
			Q213	0	0	0	Q214	1	1	0	Q214	1	1	0
G34	G34	G21	P138	0	0	0	P139	0	1	0	P139	0	1	0
	Q35	S22					Y135	0	2	0	R215	2	0	0
							R215	2	1	0				
Q36	Q36	Q23	A137	0	0	0	Y135	0	1	0	Y135	0	1	0
			K166	0	0	0	A138	0	2	0	A138	0	2	0
							C164	0	3	0	C164	0	3	0
							K167	1	1	0	K167	0	2	0
F37	F37	F24	F67	0	0	0	F68	0	0	1	F68	0	0	1
			Y134	0	0	0	Y135	1	1	2	Y135	1	1	1
			F135	0	0	0								
			R239	0	0	0								
			R290	0	0	0								
			Total	0	10	5	Total	9	24	9	Total	5	21	5

Bold type indicates symmetry-related proteins. Selection criterion based on a distance of 3.6 Å.
[a] Res., residue; P, polar; V, van der Waals; H, hydrophobic.

domain 0 (Table 3). These results demonstrate that the nature of the internal J protein mediates the surface properties of the virus, such as attachment efficiency to host cells and diffusion properties in native gels, possibly by controlling the "breathing" of the capsid.

Materials and Methods

Construction and characterization of chimeric particles

Chimeric α3 and G4 particles packaged with the ϕX174 J protein were generated by propagating *amJ* mutants in *recA*$^-$ cells containing a clone of the ϕX174 J gene.[23] The construction of the ϕX174, G4, and α3 *amJ* mutants and protein expression vectors have been described.[25,31] The infection conditions, α3 mutants, and the cell line used to produce chimeric α3 particles for crystallization were identical with those used for α3 procapsid production, except for the presence of the cloned ϕX174 J gene.[18] The assays used to characterize the chimeric particles, buoyant density centrifugation, native gel migration, and host cell attachment have been described.[16,24]

Chimera virion purification and crystallization

The chimeric virion was purified using the protocol described for the wild-type virion.[18] Crystals were obtained in sitting drops by incubation after combining an equal volume of virus sample at 6.7 mg/ml with well solution (4–7% (w/v) PEG8000, 100 mM sodium citrate (pH 5.0), 40% (v/v) glycerol, 0.02% (w/v) sodium azide, 0.1% (v/v) β-mercaptoethanol, 0.9 M NaCl) after incubation at 45 °C overnight. The chimeric α3 crystals were stable at 25 °C and could be stored at room temperature prior to data collection.

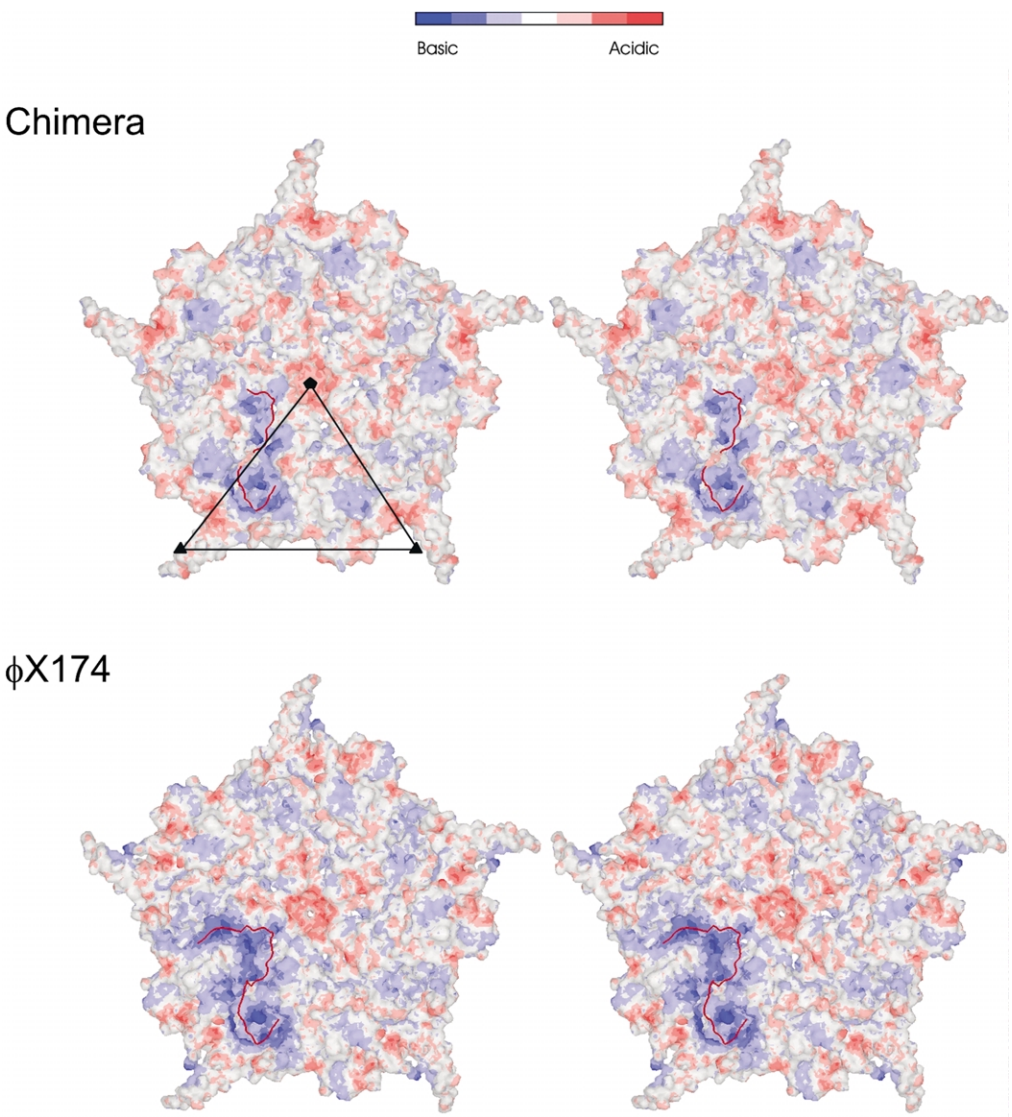

Figure 7. Stereo representation of the inner surface of an F capsid protein pentamer illustrating the effect of J binding. The electrostatic potential of the inner surface of F is shown in the absence of J everywhere except where marked on the left side of the icosahedral asymmetric unit. When J is bound the F surface becomes more basic, as shown on the left side of the icosahedral asymmetric unit.

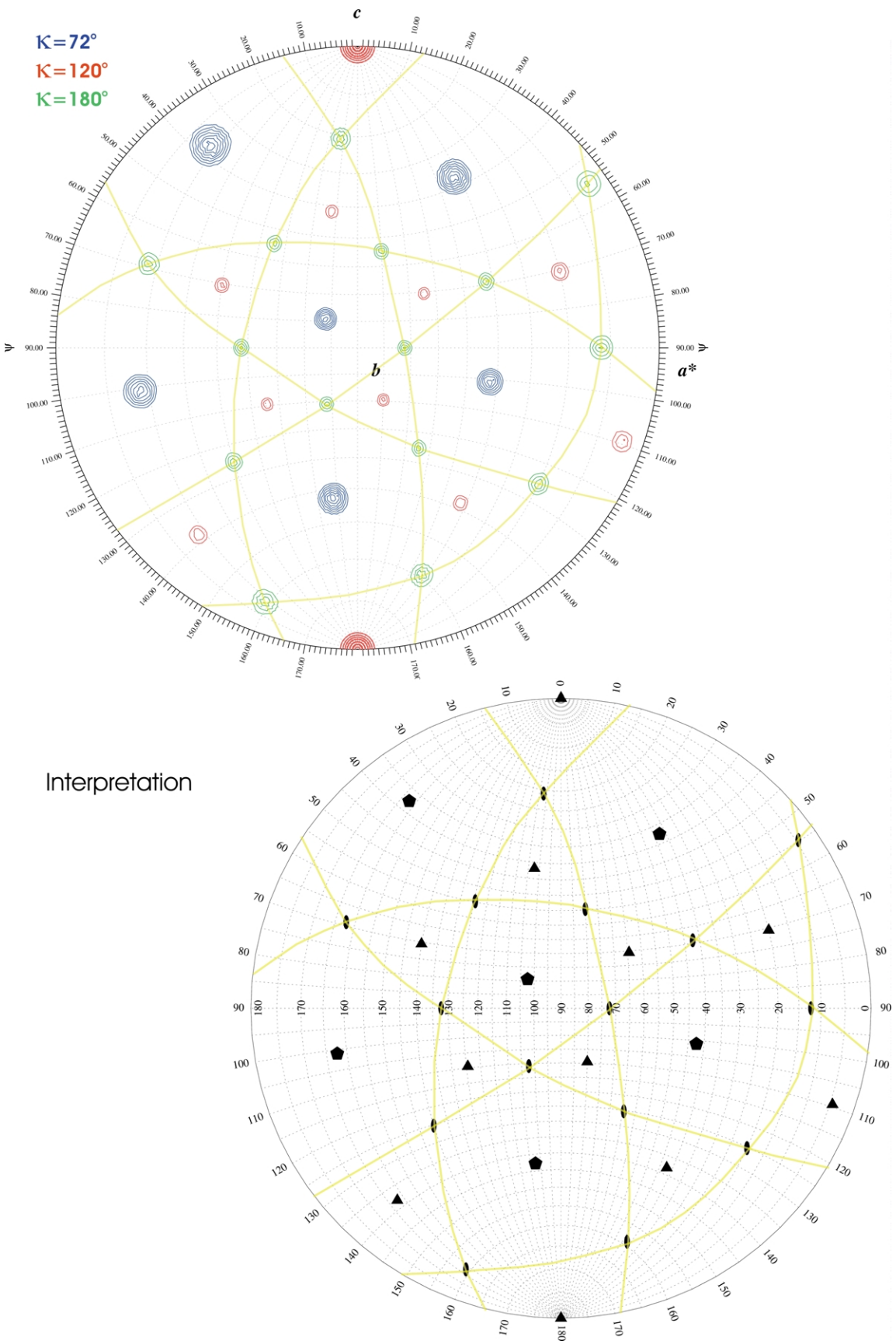

Figure 8. Self-rotation function of chimeric bacteriophage α3 using 10–6 Å resolution data. The self-rotation functions for $\kappa = 72°$, 120°, 180° are shown in a stereographic projection (top panel). The lower panel is the interpretation of the self-rotation function. Great circles are drawn to connect 2-fold axes of symmetry.

Data collection

X-ray diffraction data were collected by oscillation photography at the BioCARS beam line 14 BM-c of the Advanced Photon Source (APS). A single frozen (~100 K) crystal was used to collect 150° of data on a Quad4 CCD detector with a crystal-to-detector distance of 300 mm. Each image was exposed for 60 seconds with an oscillation angle of 0.25°. Initial indexing showed the crystal might be rhombohedral with hexagonal cell dimensions of $a = 295.1$ Å and $c = 678.2$ Å. The Matthews' coefficient,[32] V_M, was 2.7 Å^3 Da^{-1} when three particles were assumed to be in the hexagonal unit cell.

Indexing and scaling

Images were processed with the program DENZO[33] and scaled together using the program SNP,[34] confirming that the space group was *R*3. The final R_{merge} was 9.7% for all the data (15.7% in the highest-resolution bin), and the overall completeness of the data set was 60% (21% in the highest-resolution range) after removal of reflections with less that 4σ.

Orientation and position of the virion in the unit cell

With three particles in the unit cell, each particle must be located on a crystallographic 3-fold axis. One particle can be arbitrarily chosen to coincide with the origin of the unit cell. Hence, the only unknown parameter is the orientation of the origin particle around the crystallographic 3-fold axis. This orientation was determined with a self-rotation function using the program GLRF[35] with 10–6 Å resolution data, where about 10% of the large terms were used to represent the second Patterson.[36] The radius of integration was set to 150 Å, and the interpolation grid around each rotated, non-integral, reciprocal lattice point was 3 × 3 × 3. The function was explored using spherical polar coordinates stepped in intervals of 2°. The κ = 72°, 120°, 144°, and 180° sections showed that the orientation of a particle aligned with the crystallographic *c* axis was rotated by 12.5° about the *c* axis from a position where one of the icosahedral 2-fold axes would be parallel with the crystallographic *a* axis (Figure 8).

Molecular replacement

The chimeric α3 virion structure was determined to 3.5 Å resolution by molecular replacement real-space averaging using the program ENVELOPE.[37] Phases were generated to 3.5 Å resolution using the native α3 virion as a model, given the known orientation of the chimeric α3 particle in the *R*3 unit cell. An initial envelope was defined by an outer radius of 170 Å and an inner radius of 80 Å. After 14 cycles of non-crystallographic symmetry (NCS) averaging using the 20-fold redundancy, the mean correlation coefficient between the calculated and observed structure amplitudes converged to a value of 0.88 (0.61 in the outermost-resolution shell) and an overall *R*-factor of 0.17 (0.27).

Model building and refinement

The resulting averaged 3.5 Å electron density map was used to trace the C^{α} atoms for the α3 F, G, and J polypeptide chains using the program O.[38] The electron density could be interpreted in terms of the known amino acid sequences with the exception of 11 residues in the J protein. The subsequent structure was refined using two cycles of simulated annealing followed by four cycles of strict NCS conjugate gradient minimization and one cycle of grouped *B*-factor refinement using the program CNS.[39] The final *R*-factor was 0.19 (0.27) with all of the residues in the favored regions of the Ramachandran plot as calculated by the program PROCHECK.[40] Because of the 20-fold NCS redundancy, there was less than 0.2% difference between $R_{working}$ and R_{free}.

Figure drawing

Figures were generated using the graphics programs VMD,[41] MOLSCRIPT,[42] Bobscript,[43] and Raster 3D.[44]

Protein Data Bank accession code

The coordinates of the crystallographically determined chimeric α3 virion have been deposited with the RCSB Protein Data Bank with accession code 1RB8.

Acknowledgements

We thank Cheryl Towell and Sharon Wilder for their help in the preparation of this manuscript. We thank the BioCARS staff at the Advanced Photon Source for providing outstanding support at their X-ray data collection facilities. This research was supported by a GAANN fellowship to R.A.B., NSF grant MCB-9986266 to M.G.R., and NSF grant MCB-0234976 to B.A.F.

References

1. Larson, S. B., Day, J., Greenwood, A. & McPherson, A. (1998). Refined structure of satellite tobacco mosaic virus at 1.8 Å resolution. *J. Mol. Biol.* **277**, 37–59.
2. Fox, J. M., Wang, G., Speir, J. A., Olson, N. H., Johnson, J. E., Baker, T. S. & Young, M. J. (1998). Comparison of the native CCMV virion with *in vitro* assembled CCMV virions by cryoelectron microscopy and image reconstruction. *Virology*, **244**, 212–218.
3. Choi, Y. G. & Rao, A. L. (2000). Packaging of tobacco mosaic virus subgenomic RNAs by brome mosaic virus coat protein exhibits RNA controlled polymorphism. *Virology*, **275**, 249–257.
4. Fisher, A. J. & Johnson, J. E. (1993). Ordered duplex RNA controls capsid architecture in an icosahedral animal virus. *Nature*, **361**, 176–179.
5. Anderson, C. W., Young, M. E. & Flint, S. J. (1989). Characterization of the adenovirus 2 virion protein, mu. *Virology*, **172**, 506–512.
6. Davis, N. L. & Rueckert, R. R. (1972). Properties of a ribonucleoprotein particle isolated from Nonidet P-40-treated Rous sarcoma virus. *J. Virol.* **10**, 1010–1020.
7. Copeland, T. D., Morgan, M. A. & Oroszlan, S. (1984). Complete amino acid sequence of the basic

nucleic acid binding protein of feline leukemia virus. *Virology*, **133**, 137–145.
8. Chen, Z. G., Stauffacher, C., Li, Y., Schmidt, T., Bomu, W., Kamer, G. *et al.* (1989). Protein–RNA interactions in an icosahedral virus at 3.0 Å resolution. *Science*, **245**, 154–159.
9. Rossmann, M. G. & Johnson, J. E. (1989). Icosahedral RNA virus structure. *Annu. Rev. Biochem.* **58**, 533–573.
10. Vriend, G., Verduin, B. J. & Hemminga, M. A. (1986). Role of the N-terminal part of the coat protein in the assembly of cowpea chlorotic mottle virus. A 500 MHz proton nuclear magnetic resonance study and structural calculations. *J. Mol. Biol.* **191**, 453–460.
11. Wikoff, W. R., Tsai, C. J., Wang, G., Baker, T. S. & Johnson, J. E. (1997). The structure of cucumber mosaic virus: cryoelectron microscopy, X-ray crystallography, and sequence analysis. *Virology*, **232**, 91–97.
12. Tang, L., Johnson, K. N., Ball, L. A., Lin, T., Yeager, M. & Johnson, J. E. (2001). The structure of pariacoto virus reveals a dodecahedral cage of duplex RNA. *Nature Struct. Biol.* **8**, 77–83.
13. Agbandje-McKenna, M., Llamas-Saiz, A. L., Wang, F., Tattersall, P. & Rossmann, M. G. (1998). Functional implications of the structure of the murine parvovirus, minute virus of mice. *Structure*, **6**, 1369–1381.
14. Chapman, M. S. & Rossmann, M. G. (1995). Single-stranded DNA–protein interactions in canine parvovirus. *Structure*, **3**, 151–162.
15. McKenna, R., Xia, D., Willingmann, P., Ilag, L. L., Krishnaswamy, S., Rossmann, M. G. *et al.* (1992). Atomic structure of single-stranded DNA bacteriophage ϕX174 and its functional implications. *Nature*, **355**, 137–143.
16. Hafenstein, S. & Fane, B. A. (2002). ϕX174 genome–capsid interactions influence the biophysical properties of the virion: evidence for a scaffolding-like function for the genome during the final stages of morphogenesis. *J. Virol.* **76**, 5350–5356.
17. Hayashi, M., Aoyama, A., Richardson, D. L. & Hayashi, M. N. (1988). Biology of the bacteriophage ϕX174. In *The Bacteriophages* (Calendar, R., ed.), pp. 1–71, Plenum Press, New York.
18. Bernal, R. A., Hafenstein, S., Olson, N. H., Bowman, V. D., Chipman, P. R., Baker, T. S. *et al.* (2003). Structural studies of bacteriophage α3 assembly. *J. Mol. Biol.* **325**, 11–24.
19. McKenna, R., Ilag, L. L. & Rossmann, M. G. (1994). Analysis of the single-stranded DNA bacteriophage ϕX174, refined at a resolution of 3.0 Å. *J. Mol. Biol.* **237**, 517–543.
20. Dokland, T., McKenna, R., Ilag, L. L., Bowman, B. R., Incardona, N. L., Fane, B. A. & Rossmann, M. G. (1997). Structure of a viral procapsid with molecular scaffolding. *Nature*, **389**, 308–313.
21. Dokland, T., Bernal, R. A., Burch, A., Pletnev, S., Fane, B. A. & Rossmann, M. G. (1999). The role of scaffolding proteins in the assembly of the small, single-stranded DNA virus ϕX174. *J. Mol. Biol.* **288**, 595–608.
22. Fujisawa, H. & Hayashi, M. (1976). Gene A product of ϕX174 is required for site-specific endonucleolytic cleavage during single-stranded DNA synthesis *in vivo*. *J. Virol.* **19**, 416–424.
23. Jennings, B. & Fane, B. A. (1997). Genetic analysis of the ϕX174 DNA binding protein. *Virology*, **227**, 370–377.
24. Hafenstein, S. L., Chen, M. & Fane, B. A. (2004). Genetic and functional analyses of the ϕX174 DNA binding protein: the effects of substitutions for amino acid residues that spatially organize the two DNA binding domains. *Virology*, **318**, 204–213.
25. Fane, B. A., Head, S. & Hayashi, M. (1992). Functional relationship between the J proteins of bacteriophages ϕX174 and G4 during phage morphogenesis. *J. Bacteriol.* **174**, 2717–2719.
26. Serwer, P. & Pichler, M. E. (1978). Electrophoresis of bacteriophage T7 and T7 capsids in agarose gels. *J. Virol.* **28**, 917–928.
27. Spindler, K. R. & Hayashi, M. (1979). DNA synthesis in *Escherichia coli* cells infected with gene H mutants of bacteriophage ϕX174. *J. Virol.* **29**, 973–982.
28. Kodaira, K. & Taketo, A. (1984). Isolation and some properties of bacteriophage alpha3 gene J mutant. *Mol. Gen. Genet.* **195**, 541–543.
29. Kodaira, K., Nakano, K. & Taketo, A. (1985). Function and structure of microvirid phage alpha 3 genome. DNA sequence of H gene and properties of missense H mutant. *Biochim. Biophys. Acta*, **825**, 255–260.
30. Lewis, J. K., Bothner, B., Smith, T. J. & Siuzdak, G. (1998). Antiviral agent blocks breathing of the common cold virus. *Proc. Natl Acad. Sci. USA*, **95**, 6774–6778.
31. Burch, A. D. & Fane, B. A. (2000). Efficient complementation by chimeric *Microviridae* internal scaffolding proteins is a function of the COOH-terminus of the encoded protein. *Virology*, **270**, 286–290.
32. Matthews, B. W. (1968). Solvent content of protein crystals. *J. Mol. Biol.* **33**, 491–497.
33. Otwinowski, Z. & Minor, W. (1997). Processing of X-ray diffraction data collected in oscillation mode. *Methods Enzymol.* **276**, 307–326.
34. Bolotovsky, R., Steller, I. & Rossmann, M. G. (1998). The use of partial reflections for scaling and averaging X-ray area detector data. *J. Appl. Crystallog.* **31**, 708–717.
35. Tong, L. & Rossmann, M. G. (1997). Rotation function calculations with GLRF program. *Methods Enzymol.* **276**, 594–611.
36. Tollin, P. & Rossmann, M. G. (1966). A description of various rotation function programs. *Acta Crystallog.* **21**, 872–876.
37. Rossmann, M. G., McKenna, R., Tong, L., Xia, D., Dai, J., Wu, H. *et al.* (1992). Molecular replacement real-space averaging. *J. Appl. Crystallog.* **25**, 166–180.
38. Jones, T. A., Zou, J. Y., Cowan, S. W. & Kjeldgaard, M. (1991). Improved methods for binding protein models in electron density maps and the location of errors in these models. *Acta Crystallog. sect. A*, **47**, 110–119.
39. Brunger, A. T., Adams, P. D., Clore, G. M., DeLano, W. L., Gros, P., Grosse-Kunstleve, R. W. *et al.* (1998). Crystallography & NMR system: a new software suite for macromolecular structure determination. *Acta Crystallog. sect. D*, **54**, 905–921.
40. Collaborative Computational Project Number 4 (1994). The CCP4 suite: programs for protein crystallography. *Acta Crystallog. sect. D*, **50**, 760–763.
41. Humphrey, W., Dalke, A. & Schulten, K. (1996). VMD: visual molecular dynamics. *J. Mol. Graph.* **14**, 27–38.
42. Kraulis, P. J. (1991). MOLSCRIPT: a program to produce both detailed and schematic plots of protein structures. *J. Appl. Crystallog.* **24**, 946–950.
43. Esnouf, R. M. (1999). Further additions to MolScript version 1.4, including reading and contouring of

electron-density maps. *Acta Crystallog. sect. D*, **55**, 938–940.
44. Merritt, E. A. & Bacon, D. J. (1997). Raster3D: photo-realistic molecular graphics. *Methods Enzymol.* **277**, 505–524.
45. Fujisawa, H. & Hayashi, M. (1977). Assembly of bacteriophage ϕX174: identification of a virion capsid precursor and proposal of a model for the functions of bacteriophage gene products during morphogenesis. *J. Virol.* **24**, 303–313.
46. Mukai, R., Hamatake, R. K. & Hayashi, M. (1979). Isolation and identification of bacteriophage ϕX174 prohead. *Proc. Natl Acad. Sci. USA*, **76**, 4877–4881.
47. Siden, E. J. & Hayashi, M. (1974). Role of the gene beta-product in bacteriophage ϕX174 development. *J. Mol. Biol.* **89**, 1–16.

Edited by I. Wilson

(Received 8 December 2003; received in revised form 11 February 2004; accepted 11 February 2004)